Monthly Notices of the ROYAL ASTRONOMICAL SOCIETY

MNRAS **529,** L175–L180 (2024) https://doi.org/10.1093/mnrasl/slae016
Advance Access publication 2024 February 9

Discovery of a nova super-remnant cavity surrounding RS Ophiuchi

M. W. Healy-Kalesh [1]★ M. J. Darnley [1] É. J. Harvey [1,2] and A. M. Newsam[1]

[1]*Astrophysics Research Institute, Liverpool John Moores University, Liverpool L3 5RF, UK*
[2]*UK Astronomy Technology Centre, STFC, Royal Observatory, Edinburgh EH9 3HJ, UK*

Accepted 2024 February 8. Received 2024 February 6; in original form 2023 September 5

ABSTRACT

The prototypical nova super-remnant (NSR) was uncovered around the most rapidly recurring nova (RN), M31N 2008-12a. Simulations of the growth of NSRs revealed that these large structures should exist around all novae, whether classical or recurrent. NSRs consist of large shell-like structures surrounding excavated cavities. Predictions, informed by these simulations, led to the discovery of an extended cavity coincident with the Galactic RN, RS Ophiuchi (RS Oph), in far-infrared archival *IRAS* images. We propose that this cavity is associated with RS Oph and is therefore evidence of another NSR to be uncovered.

Key words: hydrodynamics – stars: individual RS Oph – novae, cataclysmic variables – ISM: general.

1 INTRODUCTION

Recurrent novae (RNe) are a subtype of cataclysmic variables that host an accreting white dwarf (WD) within a close binary system (Walker 1954). RNe exhibit non-terminal thermonuclear driven eruptions (Starrfield et al. 1972, 2020) where the inter-eruption timescale is less than a century. During a nova eruption, much of the accreted material is ejected from the surface of the WD (Starrfield et al. 2020) at velocities of hundreds to thousands of kilometres per second (O'Brien et al. 2001). This ejected material can lead to the formation of subparsec nova shells, (see e.g. Bode, O'Brien & Simpson 2004; Shara et al. 2007, 2012; Harvey et al. 2016). A proportion of the accreted material may remain to grow the WD (Yaron et al. 2005; Hachisu, Kato & Luna 2007; Hillman et al. 2015, 2016; Kato, Saio & Hachisu 2015; Starrfield et al. 2021) towards the Chandrasekhar limit: potentially leading to a Type Ia supernova (Whelan & Iben 1973; Hachisu et al. 1999a; Hachisu, Kato & Nomoto 1999b; Hillebrandt & Niemeyer 2000).

A nova super-remnant (NSR) is a vast extended shell surrounding an RN formed by the cumulative effect of eruptions sweeping up local interstellar medium (ISM) over the lifetime of the system (Darnley et al. 2019). The first NSR found is located around the annually erupting RN, M31N 2008-12a (12a; see Darnley et al. 2016; Darnley & Henze 2020; Darnley 2021); 12a is predicted to reach the Chandrasekhar limit in less than 20 kyr (Darnley et al. 2017). Initially observed in 1992 within a H α survey (Walterbos & Braun 1992), this NSR was 'rediscovered' and associated with 12a in 2014 (Darnley et al. 2015). The 12a NSR is substantially larger than any other nova shell, with semiminor and semimajor axes extending to 90 and 134 pc, respectively (Darnley et al. 2019), rivalling the sizes of the largest known supernova remnants (Stil & Irwin 2001).

A preliminary study with one-dimensional hydrodynamical simulations (using MORPHEUS; Vaytet, O'Brien & Bode 2007) demonstrated the viability of NSR formation and persistence over the lifetime of a nova system. Healy-Kalesh et al. (2023a) presented an extensive suite of one-dimensional hydrodynamical simulations exploring the impact of accretion rate, WD temperature and initial mass, and ISM density on NSR evolution. The Healy-Kalesh et al. (2023a) study included the evolution of WD mass and the subsequent impact on ejecta properties, and incorporated radiative cooling. All Healy-Kalesh et al. (2023a) NSRs consisted of a very low density excavated cavity surrounded by a hot ejecta pile-up region all contained within a thin, high-density shell of swept-up ISM.

Darnley et al. (2019) and Healy-Kalesh et al. (2023a) demonstrated that dynamic NSRs should form around all nova systems, including classical novae (Darnley & Henze 2020; Darnley 2021). Furthermore, NSRs can exist around novae with growing *or eroding* WDs, indicating that NSRs should surround old novae with low-mass WDs as well as RNe (Healy-Kalesh et al. 2023a). Recently, a second NSR has been discovered around the Galactic RN, KT Eridani, through detection of its H α shell (Shara et al. 2023; Healy-Kalesh et al. 2023b). A survey of M31 and LMC RNe did not find evidence for other NSRs (Healy-Kalesh, Darnley & Shara 2024). Although such a dearth of NSRs may be due to the lower intrinsic luminosity of NSRs around systems with longer recurrence periods.

RS Ophiuchi (RS Oph) is a Galactic symbiotic RN at a distance of $1.4^{+0.6}_{-0.2}$ kpc (Barry et al. 2008) or $2.4^{+0.3}_{-0.2}$ kpc (Bailer-Jones et al. 2021), however this latter *Gaia* determination may be biased by the long-period RS Oph binary (Schaefer 2018). RS Oph hosts a WD with mass $1.2 - 1.4\,M_{\odot}$ (Mikołajewska & Shara 2017) and a giant donor (M0/2 III; Dobrzycka & Kenyon 1994; Anupama & Mikołajewska 1999). RS Oph has a substantial accretion rate to drive eruptions in 1898, 1933, 1958, 1967, 1985, 2006, and 2021 (Page et al. 2022); exhibiting a recurrence period of ∼15 yr (Darnley 2021). Eruptions in 1907 (Schaefer 2004) and 1945 (Oppenheimer & Mattei 1993) may have been missed due to Sun constraints (Mikołajewska & Shara 2017).

Very long baseline interferometry (VLBI) radio observations of RS Oph during its 1985 eruption revealed a bipolar structure at a position angle of 84° (Porcas, Davis & Graham 1987; Taylor et al. 1989). This lack of spherical symmetry was also seen in VLBI and

★ E-mail: M.W.HealyKalesh@ljmu.ac.uk

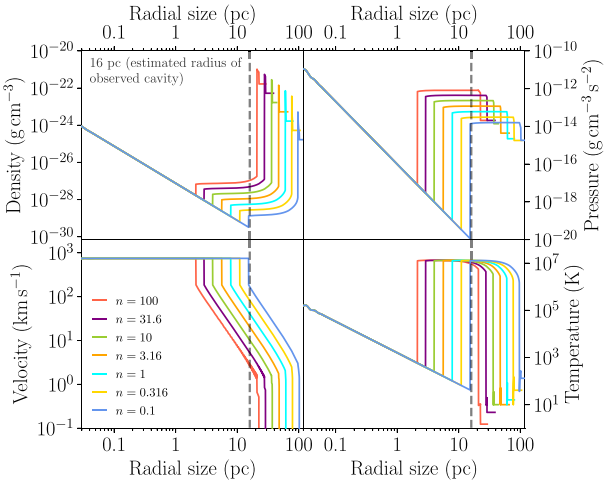

Figure 1. Simulated dynamics of the NSR surrounding RS Oph from Healy-Kalesh et al. (2023a) for different ISM densities.

Multi-Element Radio-Linked Interferometer Network (MERLIN) radio images following the 2006 eruption with collimated bipolar jet-like flows expanding toward the East–West directions (O'Brien et al. 2006; Rupen, Mioduszewski & Sokoloski 2008; Sokoloski, Rupen & Mioduszewski 2008; Mohamed, Booth & Podsiadlowski 2013). Expanding lobes with the same East–West orientation were observed in late-time *Hubble Space Telescope* (*HST*) and *Chandra* X-ray imaging after the 2006 eruption (Bode et al. 2007; Ribeiro et al. 2009; Montez et al. 2022). However, near-infrared (NIR) and X-ray observations shortly after the 2006 eruption showed ejecta expanding in a different direction to the bipolar radio structure (Lane et al. 2007; Luna et al. 2009).

As RS Oph has a short recurrence period, a massive WD, and a high accretion rate, it should be surrounded by a dynamic NSR grown over the lifetime of the system (Darnley et al. 2019; Darnley & Henze 2020; Darnley 2021; Healy-Kalesh et al. 2023a). In this letter, we present evidence for an excavated NSR cavity surrounding RS Oph. In Section 2, we predict the size of an RS Oph NSR; in Section 3, we describe the discovery of the RS Oph NSR cavity and its likely association with the nova system; the implications of uncovering another NSR are discussed in Section 4, before we present our conclusions in Section 5.

2 RS OPHIUCHI NSR MODELLING

2.1 RS Ophiuchi NSR dynamics

Healy-Kalesh et al. (2023a) presented a grid of NSRs from novae with a range of accretion rates within a range of ISM densities. Here, we utilize that grid to determine the dynamics of the NSR around an RS Oph-like system with a recurrence period of 15 yr.

We select models where a WD is grown from $1\,M_\odot$ with an accretion rate of $1 \times 10^{-7}\,M_\odot\,yr^{-1}$ within ISM ranging from $1.67 \times 10^{-25}\,g\,cm^{-3}$ ($n = 0.1$) to $1.67 \times 10^{-22}\,g\,cm^{-3}$ ($n = 100$; Runs 1–7 from Healy-Kalesh et al. 2023a). These models predict that a $1\,M_\odot$ WD takes ∼25 Myr (∼650 000 eruptions) to grow to $1.27\,M_\odot$, i.e. a recurrence period of 15 yr. We show the density, pressure, velocity, and temperature characteristics of the NSR at this stage in Fig. 1 for a range of ISM densities.

As shown in Fig. 1, NSR radial size decreases with increasing ISM density. Specifically, the outer edges of the NSR shells (and corresponding shell thicknesses) extend to 102 (5 per cent), 79 (3 per cent), 62 (2 per cent), 48 (2 per cent), 37 (3 per cent), 29 (4 per cent), and 22 pc (7 per cent) for $n = 10^{-1}$, $10^{-0.5}$, 10^{0}, $10^{0.5}$, 10^{1}, $10^{1.5}$, and 10^{2}, respectively. The velocity of the outer shell is ≲3 km s^{-1} for all NSRs and the temperature at the outer edges range from 130 K ($n = 0.1$) to 2 K ($n = 100$). The size of the NSR cavity, the innermost region, also decreases with increasing ISM density. The largest simulated cavity, ∼16 pc, occurs for $n = 0.1$. The cavity density is predicted to be up to four orders of magnitude lower than the surrounding ISM.

2.2 ISM density and NSR cavity prediction

To estimate the ISM density in the region around RS Oph, we took two approaches. The first utilizes the Besançon model of the Galaxy[1] (see e.g. Marshall et al. 2006), which provides the distribution of *K*-band extinction along different lines of sight. The second method uses the three-dimensional dusts maps[2] from Green et al. (2019). In both cases, we used the Galactic coordinates and distance to RS Oph to find the relevant grid cell containing the system. Optical extinction[3] was converted to hydrogen column density using the relation in Güver & Özel (2009), assuming Solar abundances ($X = 0.739$) (Basu & Antia 2004). The two methods yielded $n_1 = 0.032 \pm 0.001$ and $n_2 = 0.066 \pm 0.003$, respectively. While statistically inconsistent, neither method is favoured, therefore, we assume an ISM density around RS Oph of $n = 0.05 \pm 0.02$.

As the Healy-Kalesh et al. (2023a) grid does not include ISM as sparse as $n = 0.05$, we select the $n = 0.1$ model as the most suitable for predicting the current size of the RS Oph NSR shell and cavity (see Fig. 1). As such, we predict that the radius of any NSR shell surrounding RS Oph should be ≳100 pc, with the radius of the inner evacuated cavity extending to ≳15 pc. With RS Oph at a distance of $1.4^{+0.6}_{-0.2}$ kpc, this equates to an angular size of ≳250 and ≳40 arcmin for the diameters of the NSR shell and cavity, respectively. Following the methodology outlined in Healy-Kalesh et al. (2023a), we predict the total X-ray luminosity and H α luminosity from the RS Oph NSR to be $\lesssim 10^{25}$ and $\lesssim 4 \times 10^{31}$ erg s^{-1}, respectively.

3 THE SEARCH FOR A CAVITY AROUND RS OPHIUCHI

3.1 Structure in IRIS data

Given the approximate size of a potential RS Oph NSR, a search for a structure of similar dimensions was conducted in the vicinity. We concluded that the signature of an NSR cavity might be particular evident in the far-IR due to the 'missing' cool gas. The search therefore included the new generation *Infrared Astronomical Satellite* (*IRAS*) catalogue, known as IRIS (Improved Reprocessing of the *IRAS* Survey; Miville-Deschênes & Lagache 2005).

A cavity-like structure was promptly found within a 3° × 3° IRIS 100 μm image containing RS Oph (see Fig. 2). The cavity has semimajor and semiminor axes of approximately ∼40 and ∼12 arcmin, with a position angle of ∼50°. At a distance of ∼1.4 kpc (Barry et al. 2008), this equates to a physical size of ∼16 × 5 pc. While only ∼6 per cent of the size of the predicted overall NSR, this

[1] http://cdsarc.u-strasbg.fr/viz-bin/qcat?J/A+A/453/635
[2] http://argonaut.skymaps.info
[3] *K*-band extinction from the Besançon model was converted to *V*-band extinction using Cardelli, Clayton & Mathis (1989).

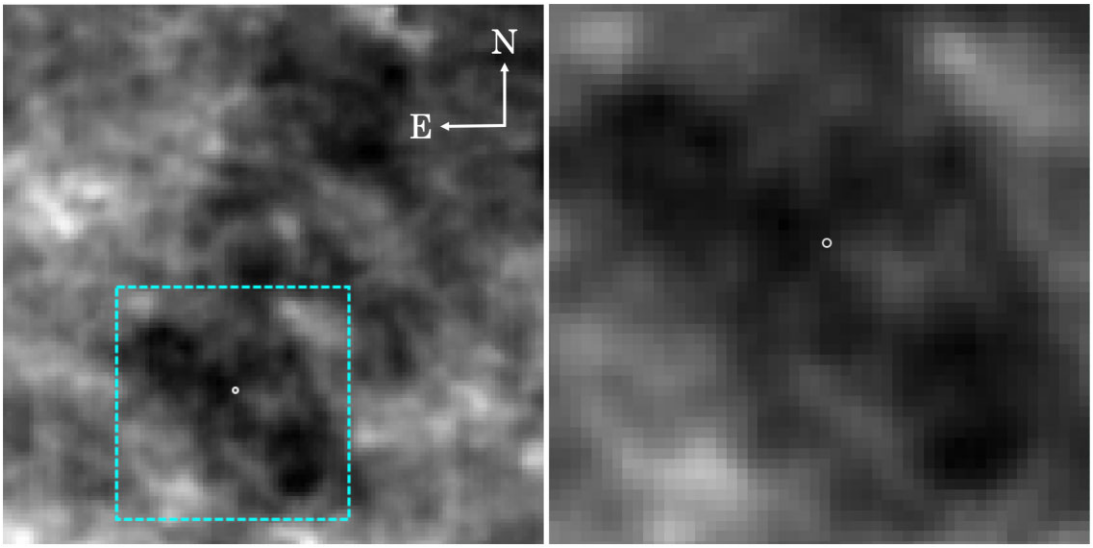

Figure 2. Cavity surrounding RS Oph. The white circles are the current location of RS Oph. *Left*: A 3° × 3° IRIS image of the surroundings of RS Oph in the far-IR (100 μm). *Right*: A 1.3° × 1.3° region from the left image (see cyan box).

is a close match to the predicted extent of NSR cavities simulated by Healy-Kalesh et al. (2023a). The sheer scale of this cavity might suggest a reason why this structure around RS Oph has not be associated with the RN until now.

3.2 Determining association between cavity and RS Oph

To confidentially associate this far-IR cavity with RS Oph, we must exclude a coincidental alignment between two unrelated phenomena. Here, we define a cavity to be any elliptical region where the flux per unit sky area is less than the flux per unit sky area within a surrounding elliptical annulus. We denote the ratio between the fluxes of the annulus and the cavity to be $\mathscr{R}$; $\mathscr{R} > 1$ defines a cavity.

3.2.1 Reference ellipse

For a reference ellipse, the ellipticity and position angle are free parameters; the position is fixed to the location of RS Oph and the semimajor axis is fixed at ∼40 arcmin (a projected size of ∼16 pc), to match the prediction of the cavity size from simulations. The inner and outer semimajor axes of the annulus are defined as 1.0 and 1.5 times the semimajor axis of the cavity.

With this reference ellipse cavity fixed at the position of RS Oph, we find that an ellipticity of 0.4 and a position angle of 45° produces the largest ratio $\mathscr{R} = 9.74$. This best-fitting cavity is illustrated in Fig. 3 (red ellipse) and thus defines our border for the cavity around RS Oph. We refer to this best-fitting ellipse as $\mathscr{E}_{\rm cavity}$.

3.2.2 Monte Carlo analysis

A Monte Carlo analysis utilized a 9° × 9° background subtracted IRIS image centred on RS Oph. We sampled ∼360 000 ellipses, each with a randomly selected semimajor axis, ellipticity, and position angle on a uniformly distributed spatial grid across the image and computed $\mathscr{R}$ at each position. The semimajor axis is taken from a range of radial sizes (∼16–22 pc) derived from linearly interpolating between $n = 0.05 \pm 0.02$ to match estimates of ISM density around RS Oph (see Section 2.2); ellipticity is taken from a range derived from the system having an inclination between 0° and 70°, and the position angle is taken from a range between 0° and 180°. The resultant distribution of the computed $\mathscr{R}$ for all the ellipses is shown in the right panel of Fig. 3 and as a heat map in Fig. 4.

We find that 97.64 per cent of the sample of ellipses (without any fixed parameters) have a ratio $\mathscr{R} < 9.74$. As such, the probability of a chance alignment of RS Oph with a cavity that has less far-IR emission than the $\mathscr{E}_{\rm cavity}$ cavity is 2.36 per cent. We note that Fig. 4 demonstrated that many positions with $\mathscr{R} > 9.74$ are in a small region near to the position of RS Oph; which further strengthens the association between the cavity and RS Oph. As $\mathscr{R}$ is determined by both the cavity and the surrounding emission, the heat map may not be a reliable source of the position of the cavity centre.

4 DISCUSSION

Having identified a large structure centred on the location of the RN RS Oph where we expect to find a vast NSR, we have explored the possibility of coincidental alignment. We found that the probability of finding a cavity-like structure such as this in the same vicinity (9° × 9°) of the sky is < 2.36 per cent and so the location of this cavity is significant.

We would expect there to be various structures within the Galactic medium with similar properties to the proposed NSR cavity surrounding RS Oph. For example superbubbles are cavities created within the ISM by the winds from OB associations (Tomisaka & Ikeuchi 1986; McCray 1988; Wright 2020). From inspection of the most well-studied OB associations provided in Wright (2020), we find that there is no superbubble spatially coincident with RS Oph (the closest being Ser OB2 with an angular radius of 31 pc; Tetzlaff et al. 2010; Mel'nik & Dambis 2017) so we rule out this as a possibility.

Other structures that can span similar areas on the sky are supernova remnants (SNRs). Cross-matching the large sample of 294 SNRs in Green (2019) with the location of our discovered RS Oph cavity reveals zero overlapping remnants as they are all confined to the Galactic plane, as do the 132 SNRs provided in the *Chandra*

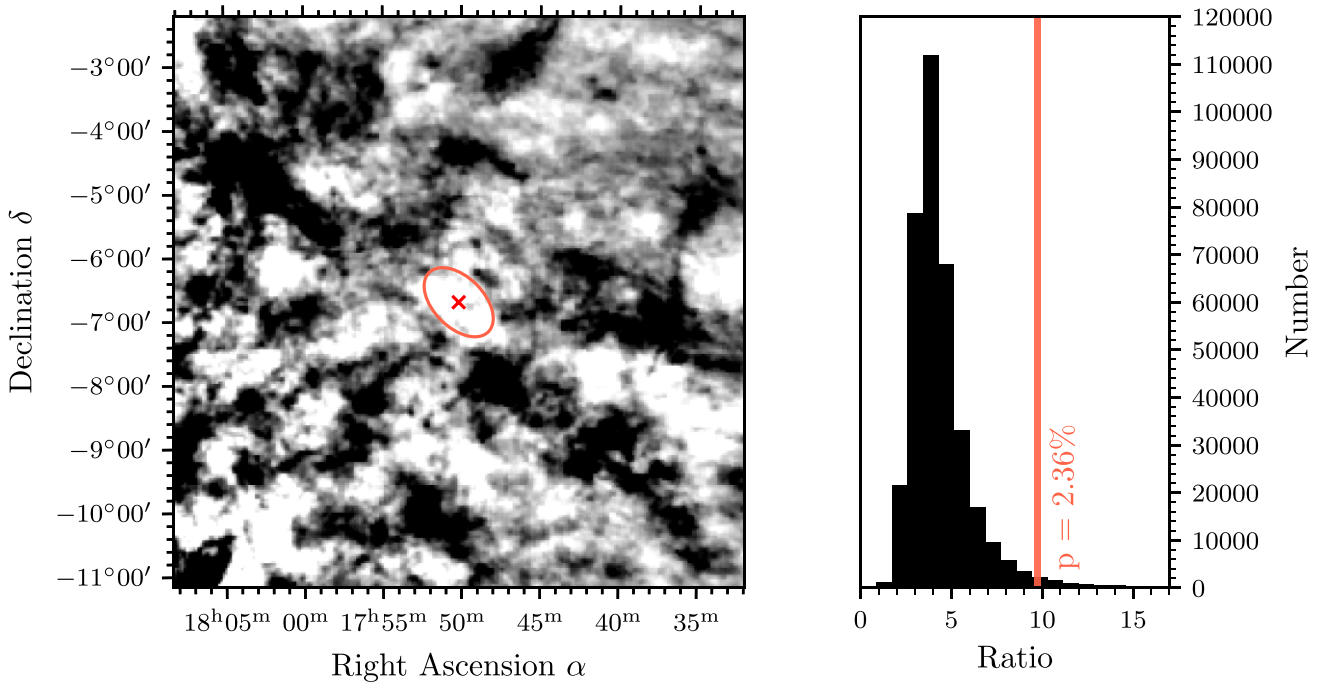

Figure 3. *Left*: An inverted 9° × 9° IRIS 100 μm centred on RS Oph (red cross). The best-fitting elliptical cavity $\mathscr{E}_{\rm cavity}$ (see the text) is illustrated by the red ellipse. *Right*: Histogram illustrating the distribution of cavity ratios $\mathscr{R}$ computed at 361 201 locations within the IRIS data (left). The horizontal red line denotes $\mathscr{E}_{\rm cavity}$.

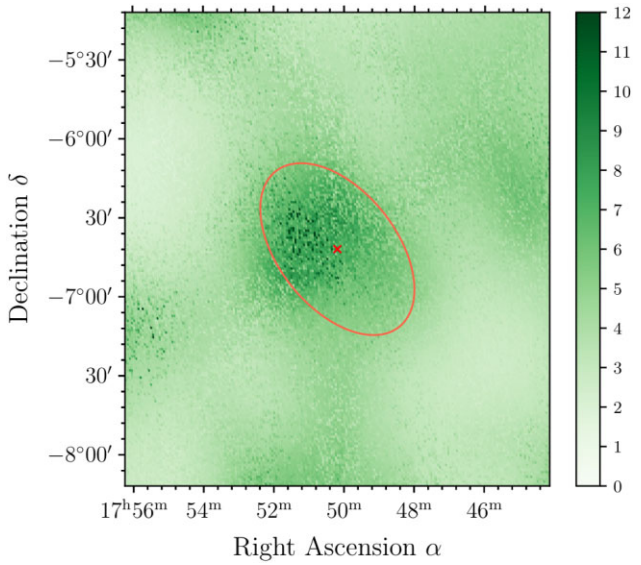

Figure 4. Heat map of ellipse ratio values $\mathscr{R}$ for the ellipse $\mathscr{E}_{\rm cavity}$ as a function of position within the IRIS data (see Fig. 3). The elliptical cavity $\mathscr{E}_{\rm cavity}$ is shown centred on the position of RS Oph.

Supernova Remnant Catalog[4] (a proportion of these SNRs are the same as those in Green 2019). A search for other sources within an approximately 20 arcmin radius of RS Oph using the SIMBAD data base (Wenger et al. 2000) displays a number of X-ray sources, including a compact object (Lin, Webb & Barret 2012), and one radio source, however none of the identified sources could be responsible for the found cavity.

We can also consider the orientation of RS Oph which has a large impact on the shaping and geometry of the shells within its immediate vicinity. The position angle of the found cavity (∼45°) does not match the value derived from the resolved shell around RS Oph created during the 2006 eruption (85°; Ribeiro et al. 2009). Yet, the cavity does resemble the general shape of a much more extended and evolved bipolar structure (O'Brien et al. 2006; Ribeiro et al. 2009) that we would expect to grow over the lifetime of RS Oph as an RN if it were consistently producing 'dumbbell-shaped' remnants (Ribeiro et al. 2009). Furthermore, the likely inhomogeneous material surrounding RS Oph at much greater distances than the immediate vicinity may contribute to the discrepancy between position angle of the cavity and the shell grown from a single eruption.

Though we have outlined (and subsequently ruled out) a number of alternative explanations for the cavity, the most compelling finding we present for its association with RS Oph is the elliptical cavity we have identified is situated with its major axis running through the location of RS Oph, with a very low probability of a coincident alignment. In fact, the cavity structure possibly associated with RS Oph can be seen in a 30° × 30° far-IR image as shown in Fig. 5. We note that there also appears to be a ring-like structure to the north-west of the elliptical cavity which may have also been shaped by RS Oph. However, we can not speculate further on this.

Uncovering a further example of an NSR through the detection of its cavity component around another RN, RS Oph, reinforces the hypothesis that these structures are created from many prior nova eruptions sweeping up the local ISM (Darnley et al. 2019; Healy-Kalesh et al. 2023a). Additionally, finding this likely NSR cavity within far-IR data encourages broadening our search for more NSRs to IR wavelengths alongside H α and X-ray emission.

[4] https://hea-www.cfa.harvard.edu/ChandraSNR/snrcat_gal.html

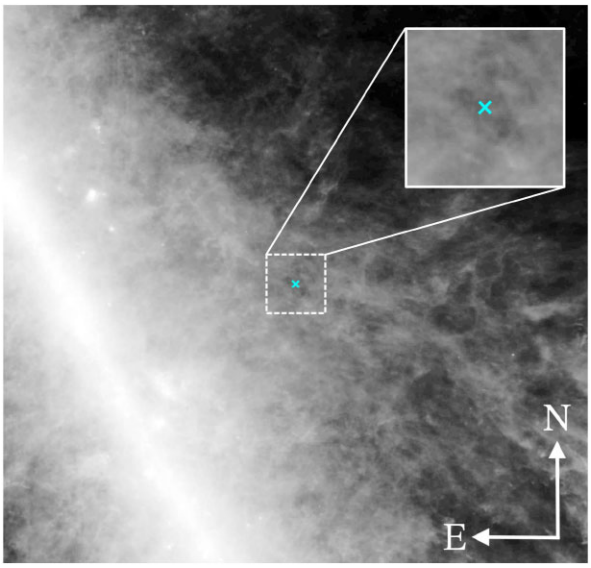

Figure 5. Cavity surrounding RS Oph can be identified in a 30° × 30° *IRAS* image. The cyan cross indicates the location of RS Oph. The white dashed-line box is a 3° × 3° region which we show in the inset.

5 CONCLUSIONS

The RN M31N 2008-12a hosts the prototypical NSR: an immense dynamically grown shell with a major axis greater than 100 pc formed from the continual sweeping of local ISM. Similar NSRs are predicted to surround other novae as it is the eruptions emanating from the central WD that drives their growth.

In far-IR *IRAS* imaging, we have uncovered the cavity of such an NSR coincident with the Galactic RN RS Oph and we find that it is very likely that they are associated. Narrow-band imaging of the surroundings of RS Oph akin to those which were employed to detect the NSR shell associated with KT Eridani (Shara et al. 2023; Healy-Kalesh et al. 2023b), would cement this connection. Ultimately, if this cavity is part of a more extended NSR, then this finding strengthens the hypothesis that all RNe should be surrounded by an NSR and further indicates that the 12a NSR is not unique.

ACKNOWLEDGEMENTS

The authors would like to gratefully thank our anonymous referee for their time spent reviewing our paper and for their constructive feedback that improved our study. MWH-K, MJD, and ÉJH recieved funding from the UK Science and Technology Facilities Council grant ST/S505559/1. The authors thank Prof. Steven Longmore for assistance estimating local ISM density. This work made use of the high performance computing facilities at Liverpool John Moores University, partly funded by LJMU's Faculty of Engineering and Technology and by the Royal Society. This research has made use of the SIMBAD data base, operated at CDS, Strasbourg, France (see Wenger et al. 2000). This research has made use of the VizieR catalogue access tool, CDS, Strasbourg, France. The original description of the VizieR service was published in Ochsenbein, Bauer & Marcout (2000).

DATA AVAILABILITY

Data in this study can be shared on reasonable request to the corresponding author. The analysis in this work made use of the PYTHON libraries: NUMPY (Harris et al. 2020) and MATPLOTLIB (Hunter 2007).

REFERENCES

Anupama G. C., Mikołajewska J., 1999, A&A, 344, 177
Bailer-Jones C. A. L., Rybizki J., Fouesneau M., Demleitner M., Andrae R., 2021, AJ, 161, 147
Barry R. K., Mukai K., Sokoloski J. L., Danchi W. C., Hachisu I., Evans A., Gehrz R., Mikolajewska J., 2008, in Evans A., Bode M. F., O'Brien T. J., Darnley M. J., eds, ASP Conf. Ser. Vol. 401, RS Ophiuchi (2006) and the Recurrent Nova Phenomenon. Astron. Soc. Pac., San Francisco, p. 52
Basu S., Antia H. M., 2004, ApJ, 606, L85
Bode M. F., O'Brien T. J., Simpson M., 2004, ApJ, 600, L63
Bode M. F., Harman D. J., O'Brien T. J., Bond H. E., Starrfield S., Darnley M. J., Evans A., Eyres S. P. S., 2007, ApJ, 665, L63
Cardelli J. A., Clayton G. C., Mathis J. S., 1989, ApJ, 345, 245
Darnley M. J., 2021, in The Golden Age of Cataclysmic Variables and Related Objects V. p. 44, preprint (arXiv:1912.13209)
Darnley M. J., Henze M., 2020, Adv. Space Res., 66, 1147
Darnley M. J. et al., 2015, A&A, 580, A45
Darnley M. J. et al., 2016, ApJ, 833, 149
Darnley M. J. et al., 2017, ApJ, 849, 96
Darnley M. J. et al., 2019, Nature, 565, 460
Dobrzycka D., Kenyon S. J., 1994, AJ, 108, 2259
Green D. A., 2019, J. Astrophys. Astron., 40, 36
Green G. M., Schlafly E., Zucker C., Speagle J. S., Finkbeiner D., 2019, ApJ, 887, 93
Güver T., Özel F., 2009, MNRAS, 400, 2050
Hachisu I., Kato M., Nomoto K., Umeda H., 1999a, ApJ, 519, 314
Hachisu I., Kato M., Nomoto K., 1999b, ApJ, 522, 487
Hachisu I., Kato M., Luna G. J. M., 2007, ApJ, 659, L153
Harris C. R. et al., 2020, Nature, 585, 357
Harvey E., Redman M. P., Boumis P., Akras S., 2016, A&A, 595, A64
Healy-Kalesh M. W., Darnley M. J., Harvey É. J., Copperwheat C. M., James P. A., Andersson T., Henze M., O'Brien T. J., 2023a, MNRAS, 521521, 3004
Healy-Kalesh M. W., Darnley M. J., Shara M. M., Lanzetta K. M., Garland J. T., Gromoll S., 2023b, preprint (arXiv:2310.17258)
Healy-Kalesh M. W., Darnley M. J., Shara M. M., 2024, MNRAS, 528, 3531
Hillebrandt W., Niemeyer J. C., 2000, ARA&A, 38, 191
Hillman Y., Prialnik D., Kovetz A., Shara M. M., 2015, MNRAS, 446, 1924
Hillman Y., Prialnik D., Kovetz A., Shara M. M., 2016, ApJ, 819, 168
Hunter J. D., 2007, Comput. Sci. Eng., 9, 90
Kato M., Saio H., Hachisu I., 2015, ApJ, 808, 52
Lane B. F. et al., 2007, ApJ, 658, 520
Lin D., Webb N. A., Barret D., 2012, ApJ, 756, 27
Luna G. J. M., Montez R., Sokoloski J. L., Mukai K., Kastner J. H., 2009, ApJ, 707, 1168
Marshall D. J., Robin A. C., Reylé C., Schultheis M., Picaud S., 2006, A&A, 453, 635
McCray R., 1988, in Roger R. S., Landecker T. L., eds, IAU Colloq. 101: Supernova Remnants and the Interstellar Medium. Cambridge University Press, Cambridge, p. 447
Mel'nik A. M., Dambis A. K., 2017, MNRAS, 472, 3887
Mikołajewska J., Shara M. M., 2017, ApJ, 847, 99
Miville-Deschênes M.-A., Lagache G., 2005, ApJS, 157, 302
Mohamed S., Booth R., Podsiadlowski P., 2013, in Di Stefano R., Orio M., Moe M., eds, Proc. IAU Symp. 281, Binary Paths to Type Ia Supernovae Explosions. p. 195
Montez R., Luna G. J. M., Mukai K., Sokoloski J. L., Kastner J. H., 2022, ApJ, 926, 100
O'Brien T. J., Davis R. J., Bode M. F., Eyres S. P. S., Porter J. M., 2001, in Schilizzi R. T., ed., Proc. IAU Symp. 205, Galaxies and their Constituents at the Highest Angular Resolutions. Proceedings of IAU Symposium, Manchester, United Kingdom, p. 260
O'Brien T. J. et al., 2006, Nature, 442, 279

Ochsenbein F., Bauer P., Marcout J., 2000, A&AS, 143, 23
Oppenheimer B., Mattei J. A., 1993, in American Astronomical Society Meeting Abstracts, #55.03
Page K. L. et al., 2022, MNRAS, 514, 1557
Porcas R. W., Davis R. J., Graham D. A., 1987, in Bode M. F., ed., RS Ophiuchi (1985) and the Recurrent Nova Phenomenon. VNU Science Press, p. 203
Ribeiro V. A. R. M. et al., 2009, ApJ, 703, 1955
Rupen M. P., Mioduszewski A. J., Sokoloski J. L., 2008, ApJ, 688, 559
Schaefer B. E., 2004, IAU Circ., 8396, 2
Schaefer B. E., 2018, MNRAS, 481, 3033
Shara M. M. et al., 2007, Nature, 446, 159
Shara M. M., Mizusawa T., Wehinger P., Zurek D., Martin C. D., Neill J. D., Forster K., Seibert M., 2012, ApJ, 758, 121
Shara M. M. et al., 2023, preprint (arXiv:2310.17055)
Sokoloski J. L., Rupen M. P., Mioduszewski A. J., 2008, ApJ, 685, L137
Starrfield S., Truran J. W., Sparks W. M., Kutter G. S., 1972, ApJ, 176, 169
Starrfield S., Bose M., Iliadis C., Hix W. R., Woodward C. E., Wagner R. M., 2020, ApJ, 895, 70
Starrfield S., Bose M., Iliadis C., Hix W. R., Woodward C. E., Wagner R. M., 2021, in The Golden Age of Cataclysmic Variables and Related Objects V. p. 30, preprint (arXiv:2006.01827)
Stil J. M., Irwin J. A., 2001, ApJ, 563, 816
Taylor A. R., Davis R. J., Porcas R. W., Bode M. F., 1989, MNRAS, 237, 81
Tetzlaff N., Neuhäuser R., Hohle M. M., Maciejewski G., 2010, MNRAS, 402, 2369
Tomisaka K., Ikeuchi S., 1986, PASJ, 38, 697
Vaytet N. M. H., O'Brien T. J., Bode M. F., 2007, ApJ, 665, 654
Walker M. F., 1954, PASP, 66, 230
Walterbos R. A. M., Braun R., 1992, A&AS, 92, 625
Wenger M. et al., 2000, A&AS, 143, 9
Whelan J., Iben Icko J., 1973, ApJ, 186, 1007
Wright N. J., 2020, New A Rev., 90, 101549
Yaron O., Prialnik D., Shara M. M., Kovetz A., 2005, ApJ, 623, 398

This paper has been typeset from a TEX/LATEX file prepared by the author.